The Azores Current System from a meridional section at 24.5°W

I. Comas-Rodríguez,[1] A. Hernández-Guerra,[1] E. Fraile-Nuez,[2] A. Martínez-Marrero,[1] V. M. Benítez-Barrios,[2] M. D. Pérez-Hernández,[1] and P. Vélez-Belchí[2]

Received 14 March 2011; revised 15 June 2011; accepted 27 June 2011; published 20 September 2011.

[1] High spatial resolution hydrographic data, including Lowered Acoustic Doppler Current Profiler (LADCP) measurements, were acquired along a meridional section at 24.5°W in October 2009. The data are analyzed in detail with the purpose of definitively defining and quantifying the zonal Azores Current System. The Azores Current and Azores Countercurrent are delimited, each extending meridionally for 110 km. The Azores Current is located between 33.5°N and 34.5°N, flanked to the north by the Azores Countercurrent (35.25°–36.25°N). Vertically, both currents reach the γ_n = 27.975 kg m^{-3} level (~2000 m depth), their mass transports ranging across thermocline as well as intermediate layers. The Azores Current transports 13.9 Sv (1 Sv = 10^6 m^3 s^{-1} ≈ 10^9 kg s^{-1}) eastward with its maximum associated with the Azores Front (33.75°N). The Azores Countercurrent flows below the surface, transporting 5.5 Sv westward. This contributes to a net eastward flow of 8.4 Sv across the section. At intermediate layers, the Azores Countercurrent transports mixed Mediterranean Water to the west, and the Azores Current transports mixed Sub-Arctic Intermediate Water to the east. Shipboard ADCP and satellite-derived geostrophic velocity are used to confirm the transports revealed by the hydrographic data.

Citation: Comas-Rodríguez, I., A. Hernández-Guerra, E. Fraile-Nuez, A. Martínez-Marrero, V. M. Benítez-Barrios, M. D. Pérez-Hernández, and P. Vélez-Belchí (2011), The Azores Current System from a meridional section at 24.5°W, *J. Geophys. Res.*, *116*, C09021, doi:10.1029/2011JC007129.

1. Introduction

[2] The Azores Current (AzC) is the northernmost current of the North Atlantic subtropical gyre (NASG). It originates as a branch of the Gulf Stream, heading southeastward and crossing the Mid-Atlantic Ridge south of the Azores [*Käse and Siedler*, 1982; *Gould*, 1985]. The AzC flows eastward as a zonal jet, associated with the Azores Front (AzF), and divides into three main branches that turn southwards [*Stramma and Siedler*, 1988; *Klein and Siedler*, 1989]. The easternmost branch feeds the Canary Current (CC) that flows across the Canary Islands [*Stramma*, 1984; *Stramma and Müller*, 1989; *New et al.*, 2001; *Machín et al.*, 2006]. The three branches feed the North Equatorial Current that flows to the west closing the NASG [*Hernández-Guerra et al.*, 2005].

[3] The eastward mass transport of the AzC has been reported to be about 10–12 Sv (1 Sv = 10^6 m^3 s^{-1} ≈ 10^9 kg s^{-1}), mainly through the upper 1000 m of the ocean [*Gould*, 1985; *Sy*, 1988; *Stramma and Müller*, 1989]. Its formation and variability have been studied both through historical data sets and circulation models [*Paillet and Mercier*, 1997; *Pingree et al.*, 1999; *Alves et al.*, 2002; *Pérez et al.*, 2003]. There are two hypotheses about the driving mechanism of the AzC. The first one is that the Azores Current is driven by the wind stress curl [*Käse and Krauss*, 1996]. The second AzC formation mechanism is believed to imply a water mass transformation associated with the Mediterranean outflow in the Gulf of Cádiz [*Jia*, 2000; *Özgökmen et al.*, 2001], relying on the dynamical concept of β-plumes. A combination of both has also been considered by *Lamas et al.* [2010], providing higher transport estimates (16.5 Sv for the first 1500 m from Argo data). The AzC variability seems to depend mainly on the magnitude of the exchange through the Strait of Gibraltar.

[4] Some studies have also demonstrated the presence of a recirculation as a westward counterflow adjacent to the AzC, called the Azores Countercurrent (AzCC) as defined by *Onken* [1993], who attributes the existence of the AzCC to a feature in the meridional gradient of the wind stress curl. [*Cromwell et al.*, 1996] used altimetry and hydrography data to indicate that such westward flow north of the AzC appears to be a persistent feature of the circulation in this region. In line with the AzC formation, two mechanisms have been suggested to drive the AzCC. *Alves and Colin de Verdière* [1999] supported an eddy-driven mechanism, which is expected to form two westward countercurrents, north and south of the AzC due to geostrophic turbulence rectification. In contrast, the second hypothesis suggests the formation of a single westward countercurrent to the north of the AzC, due to the aforementioned topographic β-plume

[1]Facultad de Ciencias de Mar, Universidad de Las Palmas de Gran Canaria, Las Palmas, Spain.
[2]Instituto Español de Oceanografía, Centro Oceanográfico de Canarias, Santa Cruz de Tenerife, Spain.

0148-0227/11/2011JC007129

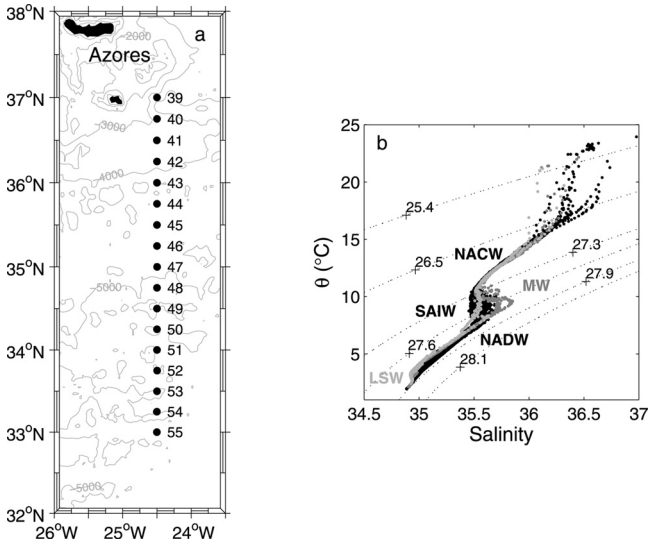

Figure 1. (a) Location of the CTD stations occupied at the Azores Current System during the ORCA cruise in the fall of 2010. For reference, 200-, 1000-, 2000-, 3000-, 4000- and 5000-m isobaths are shown [*Smith and Sandwell*, 1997]. (b) Θ-S diagram. NACW, SAIW, MW (dark gray, stations 41–43), NADW and LSW (light gray, stations 39 −43) are shown.

[*Kida et al.*, 2008; *Volkov and Fu*, 2010]. According to these studies, the resulting principal current flows westward, transporting 2–7 Sv. Also, *Fiekas et al.* [1992] observed that the initial eastward-flowing 12 Sv registered in the upper 700 m were reduced to 7 Sv when considering the adjacent counterflow. However, most of the literature focuses on modeling or limited sets of data.

[5] Several pending questions about these currents, like the observational verification of their vertical extension and the horizontal structure, demand further in-situ measuring efforts. To fulfill this objective, an extensive hydrographic data set that can be used to verify the conclusions drawn from modeling has been missing. This paper provides a high spatial resolution synoptic survey expressly designed to measure both the AzC and AzCC and resolve the mesoscale. The main aim of the present study is to delimit (both horizontally and vertically) and estimate the Azores Current System (ACS) transport across a meridional section using hydrographic data. We present a quantitative study that constitutes a reference in the hydrographic description of the water column in the region while providing a new insight into the meridional horizontal structure of the system. The paper is structured as follows. After presenting the collected hydrographic data and describing the methodology in section 2, the water mass distribution and circulation in the Azores Current System is thoroughly studied in section 3. Our final discussion is given in section 4.

2. Data and Methods

[6] The ORCA cruise was carried out between 15 October and 11 November 2009 onboard the BIO *Hespérides*. The survey comprised three large-scale sections, two zonal sections at nominal latitudes of 29° and 37°N, joined by a meridional section at the longitude of 24.5°W. In order to locate the AzC and the AzCC, we will focus on this meridional section between latitudes 37° and 33°N (stations 39–55, see Figure 1a), as will be later justified. These 17 SeaBird 911+ CTD stations were carried out with a spatial separation of 15 nm (~28 km) between 26 October and 1 November 2009. The location and spacing of these stations allow the quantification of the flow across the section. A teach cast, dual sensors of temperature and conductivity acquired data from the surface down to 15–20 m above the bottom. The temperature and pressure sensors were calibrated before the cruise at the SeaBird facilities, whereas the conductivity sensor was calibrated on board with bottle sample salinities (hereinafter salinity is expressed in the Practical Salinity Scale). Additionally, neutral density (γ_n) is computed following *Jackett and McDougall* [1997].

[7] The Lowered Acoustic Doppler Current Profiler (LADCP) system was mounted on the rosette and deployed at each CTD cast. The LADCP consists of two 300 kHz Teledyne/RDI Workhorses (WH) run in master/slave mode. The data are processed using the Visbeck software developed at Columbia University [*Fischer and Visbeck*, 1993]. Continuous current measurements were also made in the upper 700 m using a 75 kHz Ocean Surveyor Shipboard ADCP (SADCP). These data are properly calibrated and GPS-referenced, as well as processed with the CODAS (Common Ocean Data Access System) processing toolbox. The Visbeck software adjusts the shallowest LADCP data to the SADCP data and the barotropic tidal component is removed from the ADCP data. Continuous temperature records were also acquired using an SBE-21 thermosalinometer and averaged onto a 1/10° grid. The altimeter data come from the Aviso global near-real time Ssalto/Duacs merged product, which use Jason-1, Envisat, GFO, ERS-1, ERS-2 and Topex/Poseidon data. Absolute geostrophic velocities, computed from absolute dynamic topography, have been acquired on a 1/4° grid along the 24.5°W meridional section (averaging the data provided by Aviso at 24.75° and 24.25°W from 26 October to 1 November). Ocean surface wind stress data used to obtain Ekman transport come from the QuikSCAT scatterometer.

[8] Mass transport is calculated by dividing the water column into 14 neutral density layers, following the criteria proposed by *Ganachaud* [2003] for the Atlantic Ocean, but with a slight modification for central waters. Thus, each layer corresponding to thermocline waters covers roughly a depth range equivalent to the other layers. Geostrophic relative velocities are obtained using the thermal wind equation. To integrate this equation, the reference level of no-motion has been located at $\gamma_n = 28.072$ kg m^{-3} (roughly 3000 m). An estimation of the absolute velocity is obtained using LADCP data [*McDonagh et al.*, 2008] following the procedure described by *Comas-Rodríguez et al.* [2010]. This methodology involves the calculation of a reference velocity by comparing the geostrophic estimates to direct velocity measurements.

3. Results

3.1. Water Mass Distribution

[9] Potential temperature (Θ) and salinity (S) data obtained during the cruise allow water mass identification as

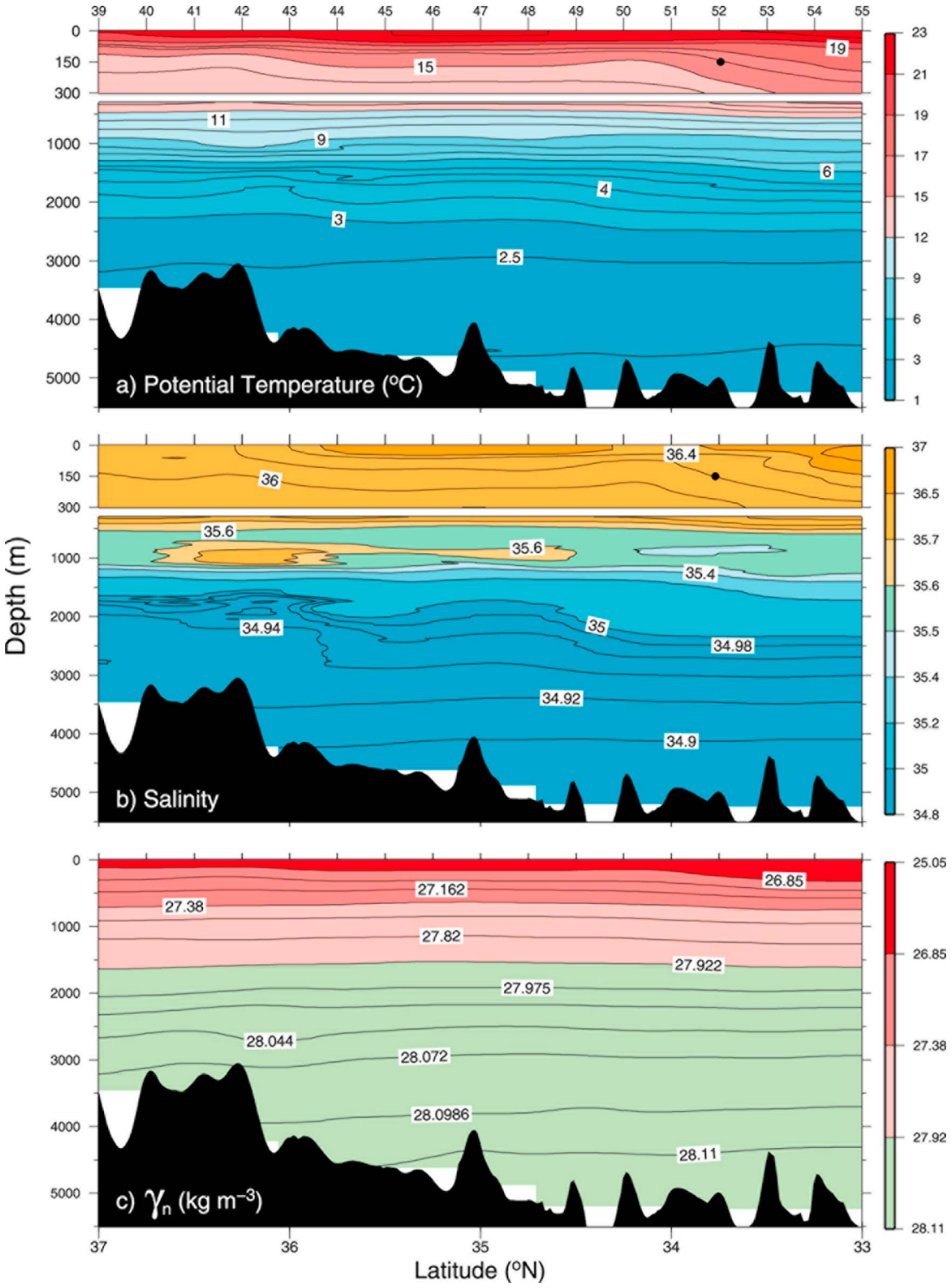

Figure 2. Vertical sections for (a) Θ (°C), (b) salinity and (c) γ_n (kg m^{-3}). Note the different vertical scales in Figures 2a and 2b. The black dots mark the location of the AzF as suggested by *Pérez et al.* [2003].

shown in Figure 1b. In this Θ-S diagram, the five main water masses present at the section are marked. A slight scattering is seen above the seasonal thermocline, due to heating, precipitation and evaporation that take place at shallow depths. Figure 2 shows Θ, salinity and γ_n vertical sections. Central waters extend to a density level of γ_n < 27.38 kg m^{-3} (roughly 700 m), and define the thermocline layer, occupied by North Atlantic Central Water (NACW). The AzF is found near station 52 (~33.75°N, marked by a black dot in Figures 2a and 2b), corresponding

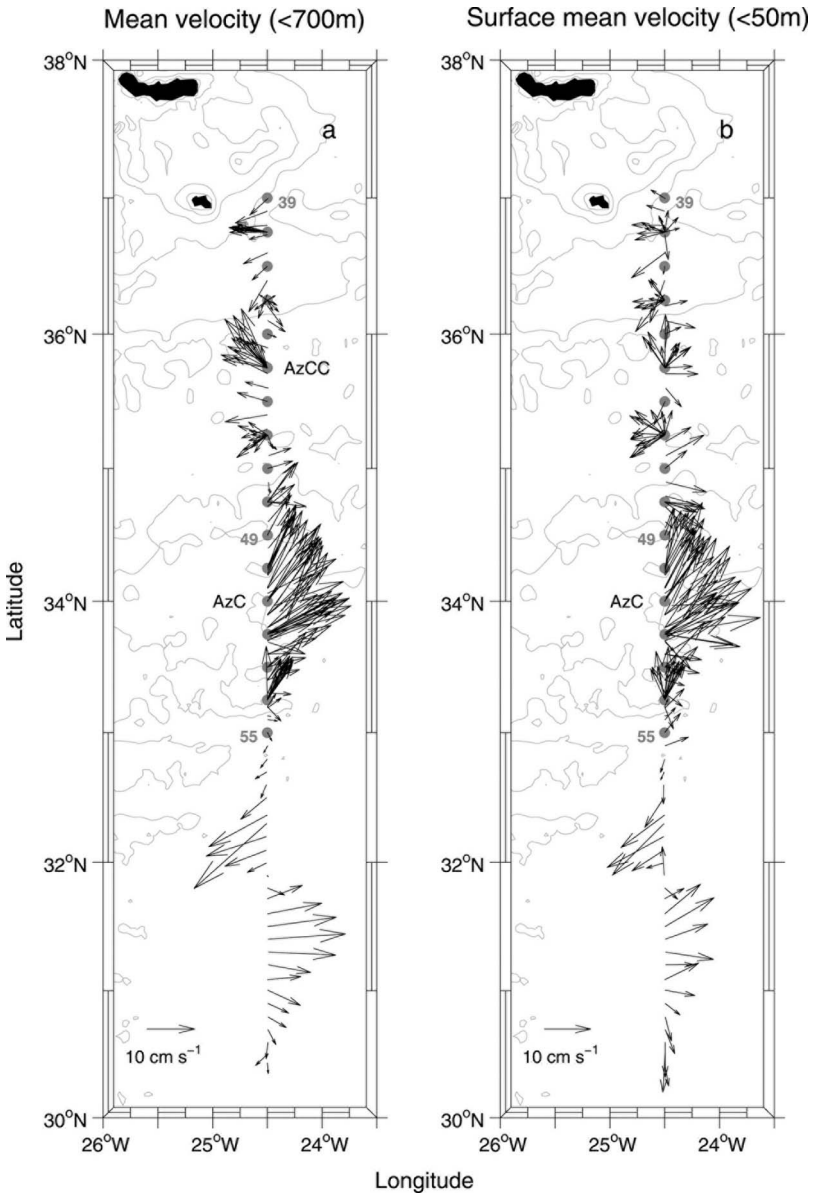

Figure 3. (a) Full-depth averaged and (b) mean surface velocities from the SADCP. For reference, locations of the CTD stations and main isobaths are shown.

to the 16.2°C isotherm and 36.2 isohaline at 150 dbar as suggested by *Pérez et al.* [2003]. In these vertical sections, temperature and salinity gradients can be seen where the AzF is located. Therefore, the AzF is associated with the maximum baroclinic velocities registered in the Azores Current. In contrast, other frontal zones such as the Cape Verde Frontal Zone (CVFZ), although known for their characteristic fluctuations of isolines [*Martínez-Marrero et al.*, 2008], are not associated with maximum velocity values. Below the central waters, at intermediate layers ($27.38 < \gamma_n < 27.922$ kg m^{-3}, roughly 700–1600 m), relatively warmer and saltier (>35.7) Mediterranean Water (MW) is found between stations 41 and 43 (dark gray in Figure 1b). In Figure 2b, this MW core (36.5°–36°N) is located at approximately 1000 m, whereas values above 35.6 spread horizontally up to station 49 (34.5°N). Between stations 50 and 53 (34.25°–33.5°N) relatively cooler and fresher (>35.5) mixed Sub-Arctic Intermediate Water (SAIW) is also found, approximately in the 700–900 m range. The upper limit of the SAIW domain is defined by *Arhan* [1990] at the 27.3 isopycnal, but 'pure' SAIW temperature and salinity values are much lower than those shown here. The deep layers, from approximately 1600 m to the ocean bottom ($\gamma_n > 27.922$ kg m^{-3}), are composed of North Atlantic Deep Water (NADW) and Labrador Seawater (LSW). LSW is found from stations 39 to 43 (light gray in Figure 1b, 37°–36°N in Figure 2). The presence of LSW is evidenced by the rise of isohalines (Figure 2b) and bending of isoneutrals (Figure 2c) below 2000 m, as well as Θ values above 2°C and salinity around 34.9 [*van Aken*, 2000].

3.2. The Azores Current and Countercurrent System

[10] In order to horizontally delimit the AzC and AzCC domains, velocity from the SADCP is shown in Figure 3.

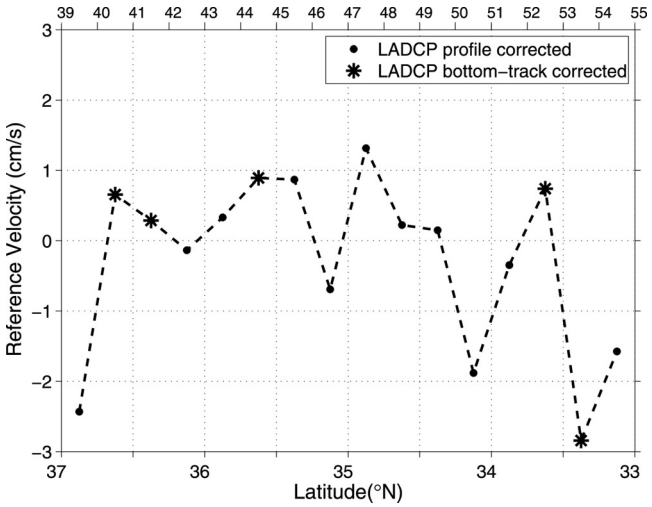

Figure 4. Reference level velocities (cm s^{-1}) obtained from LADCP bottom-track (stars) and full-depth (dots) profiles.

Velocity averaged over nearly the 700-m depth range reached by the instrument (Figure 3a) and averaged velocity up to 50 m (Figure 3b), are plotted separately for comparison. Figure 3 clearly reveals a cyclonic recirculation at the southern part of the section, at latitudes south of 33°N (station 55). Al already mentioned, this study only covers stations 39 (located at the northernmost point of the section) to 55. In the following, the transect is divided into four different sectors. From station 39 (37°N) and up to station 42 (36.25°N), a westward velocity is present which, as we will show, belongs to an anticyclonic recirculation located north of the section. Between stations 42 and 46 (36.25°–35.25°N) we find the westward-flowing AzCC at subsurface levels, unnoticeable at the surface, as shown by the lack of flow in Figure 3b. To the south, enclosed by stations 46 and 49 (35.25°–34.5°N), there is a cyclonic recirculation, apparently forced by the strong horizontal shear in this transition area. Finally, the AzC can be identified between stations 49 to 53 (34.5°–33.5°N), flowing eastward in the surface layer and below (Figures 3a and 3b).

[11] Figure 4 shows the reference velocity obtained for the section, replacing the zero-velocity at γ_n = 28.072 kg m^{-3}. Each value, corresponding to a station pair, represents the velocity applied to the geostrophic profile to match the LADCP data. As described by *Comas-Rodríguez et al.* [2010], either bottom-track or LADCP full-depth profiles are used when referencing the geostrophic calculations. Reference velocities included in the corrected transport estimates are quite small (see Figure 4). Figure 5 shows the accumulated mass transport along the section, considering surface (γ_n < 27.38 kg m^{-3}), intermediate (27.38 < γ_n < 27.922 kg m^{-3}) and deep (γ_n > 27.922 kg m^{-3}) layers separately. Ekman transport has been added to the shallowest layer. Both initial (dashed lines) and LADCP-referenced (solid lines) geostrophic accumulated transports are shown separately. The latter is calculated using the absolute velocities obtained by including the reference level velocities provided by the LADCP data. A large water volume is comprised between γ_n = 27.922 kg m^{-3} and the bottom (from approximately 1600 m to almost 5000 m depth). This causes the transport in the deep water layers to be modified by the new reference velocity, magnifying its contribution. In the following, we will discuss the flow resulting from the LADCP-referenced mass transport estimates.

[12] Figure 5 presents a quantification of the flow within the AzC and AzCC. The negative (westward) flow from stations 39 to 42 (37°–36.25°N) is caused by the westward part of an anticyclonic recirculation, as will be discussed later. Concerning the AzCC domain, between stations 42 and 46 (36.25°–35.25°N), a prominent westward flow is noticeable at surface and intermediate layers. Mass transports at both the surface (−3.4 Sv) and intermediate (−2.1 Sv) layers contribute to the AzCC, with a westward flow of 5.5 Sv. The cyclonic recirculation located south of station 46 (35.25°N) spans until station 48 (34.25°N), thereafter the mass transport is nearly zero (from surface to γ_n = 27.922 kg m^{-3}) until station 49 (34.5°N). Between stations 49 and 53 (34.5°–33.5°N), the AzC transports a total of 13.9 Sv (10.7 Sv carried at thermocline layers and 3.2 Sv at intermediate depths) eastward. With the above mentioned results, an eastward net mass transport of 8.4 Sv flows across the meridional section at 24.5°W. Figure 5 confirms that the widths of the AzC and AzCC are about 110 km each. The maximum eastward flow of the AzC is associated with the AzF, which is located near station 52 (~33.75°N) as placed in Figure 2.

[13] Figure 6 reveals the vertical structure of the AzC and AzCC from SADCP data (Figures 6a and 6b) and the calculated mass transports (Figures 6c and 6d). Both the geostrophic (dashed line) and LADCP-referenced (solid line) estimates are shown (see caption in Figure 6). A very small vertical shear in the westward velocity corresponding to the AzCC (Figure 6a) is seen between 150 m and 650 m depth, with a slight maximum registered just below the surface. Integrated mass transport in this same area (Figure 6c) show that the highest transport is located roughly between 500 and 700 m (27.162 < γ_n < 27.38 kg m^{-3}). Figure 6b shows a

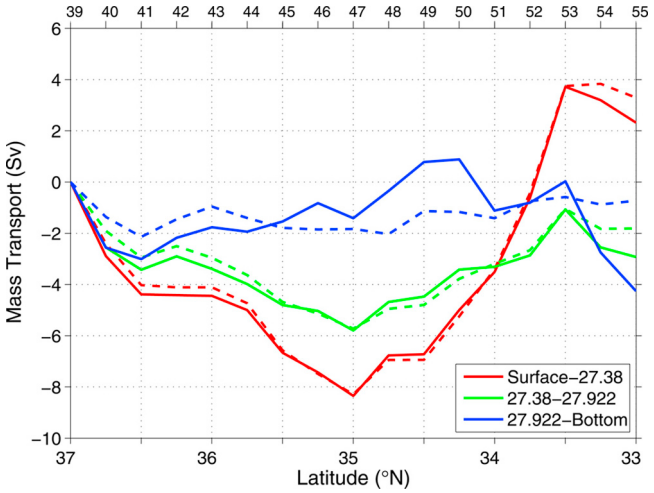

Figure 5. Accumulated geostrophic mass transport (Sv) for thermocline (red), intermediate (green) and deep (blue) layers. Dashed and solid lines show the initial and LADCP-referenced accumulated mass transports, respectively. Positive/negative values stand for eastward/westward flows.

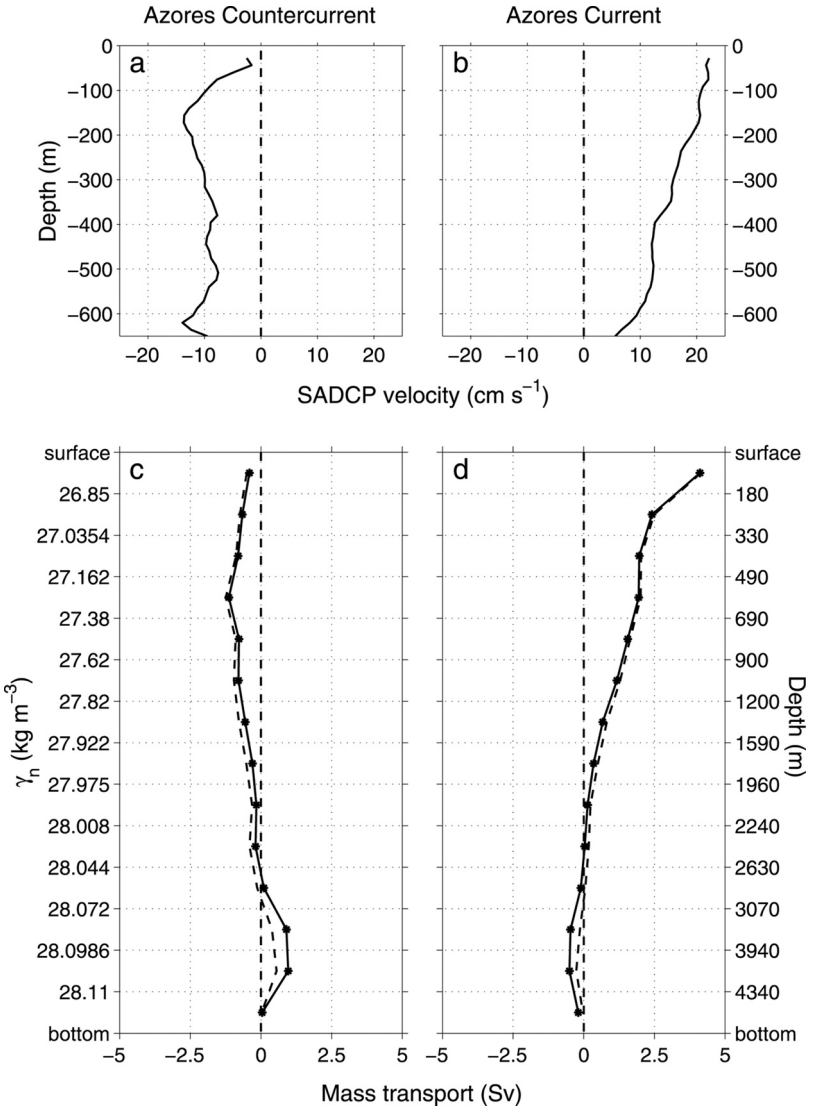

Figure 6. SADCP averaged velocities (cm s^{-1}) corresponding to the (a) AzCC and (b) AzC domains. Geostrophic mass transport (Sv) per layer for the (c) AzCC and (d) AzC. Dashed lines show the geostrophic mass transport, and solid lines stand for the LADCP-referenced mass transport.

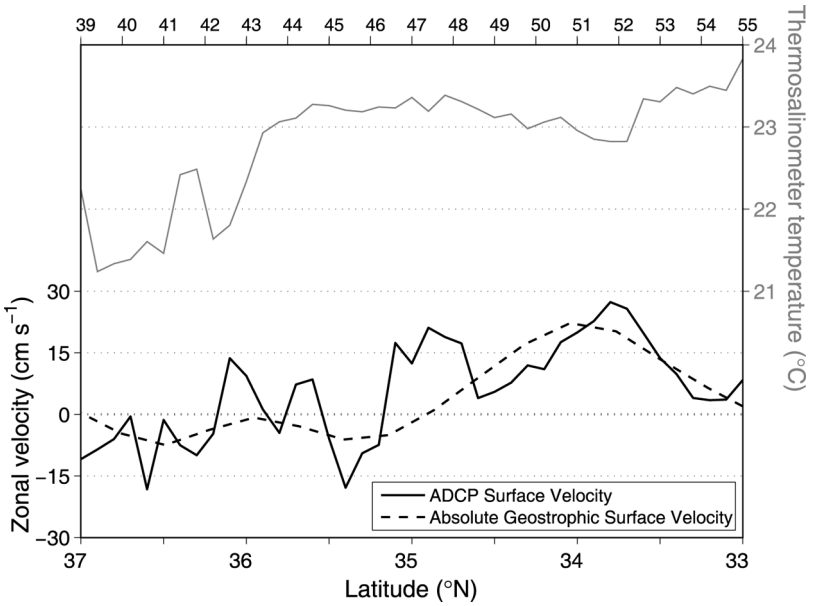

Figure 7. Surface layer data at 24.5°W. Gray line represents temperature (°C) recorded by the thermosalinometer. Black lines correspond to the zonal velocity component (cm s^{-1}) measured by the SADCP (solid) and altimeter (dashed). Note the different y-scales.

baroclinic eastward flow corresponding to the AzC, as also seen in Figure 6d. Figures 6c and 6d show significant mass transport up to approximately 2000 m, including the thermocline as well as intermediate layers (up to γ_n = 27.975 kg m^{-3}). The eastward flow seen at the deepest layers in Figure 6c is probably associated with the presence of LSW on the northern margins of the AzCC domain, also observed in Figure 1b, which flows across the section in the deepest layers.

[14] It can be appreciated in Figure 7 how the SADCP velocity measurements in the shallowest layer roughly follow the pattern provided by the satellite-derived geostrophic velocity. The AzC location is clearly observed between stations 49 and 53 (34.5°–33.5°N) and the AzF remains coincident with the peak located near station 52 (33.75°N), although the altimeter geostrophic velocity presents a shift to northern latitudes. Whereas the first layer properly reproduces the AzC, the AzCC (stations 42–46, 36.25°–35.25°N) is not shown, as observed by *Barbosa Aguiar et al.* [2011], due to the fact that the main AzCC flow takes place at subsurface depths. On the other hand, temperature records show the anticyclonic eddy signal at the northern part of the section, up to station 43 (36°N), followed by a lack of recognizable structures to the south. The AzF can be associated with the steep slope observed at station pair 52–53 (33.75°–33.5°N).

4. Discussion and Conclusions

[15] In order to identify and quantify the counter-flowing zonal large-scale currents south of the Azores archipelago, this study analyzes a hydrographic data set acquired between 37° and 33°N at 24.5°W during the ORCA cruise. Our results reveal a surface intensified AzC flanked to the north by the westward counterflow of the AzCC (as named by *Onken* [1993]). The presence of a single counterflow supports the topographic β-plume formation mechanism suggested in previous studies. We show that the AzCC spans the intermediate water depths (up to ~2000 m), reaching a greater depth than those reported by *Klein and Siedler* [1989] (800 m), *Fiekas et al.* [1992] (700 m), *Arhan et al.* [1994] (700 m) and *Paillet and Mercier* [1997] (800 m); and close to the results obtained by *Sy* [1988] (1500–2000 m) or *Tychensky et al.* [1998] (2000 m). We also find a horizontal extension of the AzCC that is similar to the AzC, both extending for about 110 km. *Tychensky et al.* [1998] reported the same horizontal extension for the AzC.

[16] The AzC transports 13.9 Sv to the east, matching that obtained by the above mentioned studies in the region. On the other hand, the AzCC carries 5.5 Sv to the west, reducing the net eastward transport across the section to 8.4 Sv. Recent model estimates suggest that a westward transport of 6.8 Sv is associated with the AzCC [*Volkov and Fu*, 2010], reaffirming the results obtained from the quality data set used here. Considering that both currents flow across the section, occupying up to ~2000 m, the observed MW is transported by the AzCC to the west (as found by *Peliz et al.* [2007]). In contrast, the SAIW that is found above 1000 m depth is transported to the east by the AzC. Future surveys in the region could be carried out to accomplish complementary sections that confirm the suspected pattern to be followed by the currents studied here.

[17] Figure 8 provides an additional view of the flow pattern of the AzC and AzCC. Accumulated mass transports per station pair are shown as bar diagrams for thermocline (γ_n < 27.38 kg m^{-3}), intermediate (27.38 < γ_n < 27.922 kg m^{-3}) and deep (γ_n > 27.922 kg m^{-3}) waters (Figures 8a, 8b,

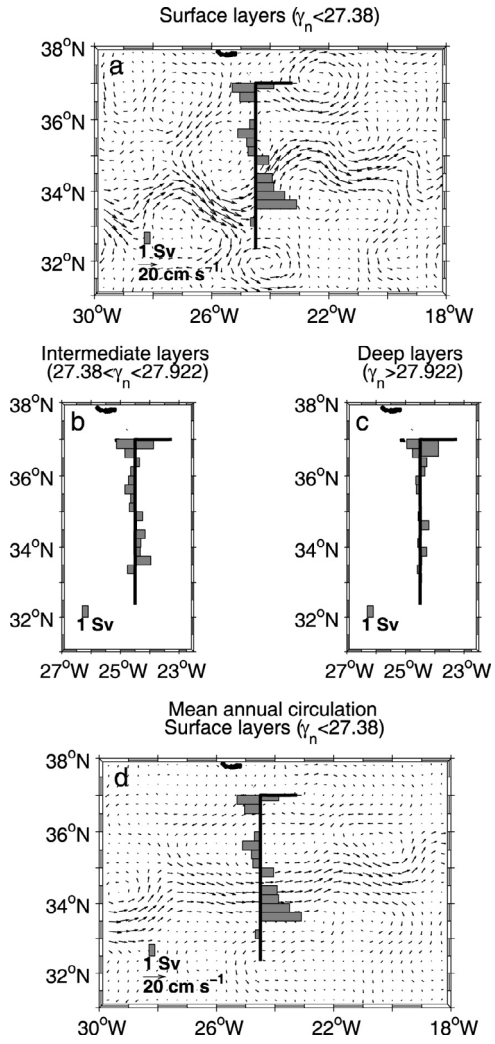

Figure 8. Vertically integrated mass transport per station pair for (a, d) thermocline, (b) intermediate and (c) deep layers. The thick black line marks the vessel path. At the surface layer, arrows represent the satellite absolute geostrophic velocity during the cruise (Figure 8a) and the mean annual circulation (Figure 8d).

and 8c). The thick solid black line marks the vessel path and we have included one extra station pair, which corresponds to the end of the northern ORCA section. The quasi-barotropic anticyclonic recirculation located north of 36.25°N is now revealed at each depth range. Southward of 36.25°N, the AzCC flows to the west (up to 35.25°N) occupying surface and intermediate layers, as seen in Figure 6c. The cyclonic recirculation south of 35.25°N is confirmed in Figures 8a and 8b. The AzC is enclosed between 34.5° and 33.5°N with an eastward mass flow down to γ_n = 27.975 kg m^{-3}, as suggested in Figure 6d. As expected, the maximum flow is associated with the AzF, located near 33.75°N. The altimeter geostrophic velocity shown in the surface layer during the time of the observations (Figure 8a) clearly reveals the AzC but not the AzCC because it flows below the surface [*Onken*, 1993; *Paillet and Mercier*, 1997]. The mean annual circulation, obtained from altimeter absolute geostrophic velocities, is observed in Figure 8d, confirming the patterns described by the hydrographic meridional section carried out at 24.5°W.

[18] **Acknowledgments.** This study has been performed thanks to the ORCA (CTM2005-04701 and CTM2008-04510) project, financed by the Spanish Government and Feder. The altimeter products were produced by Ssalto/Duacs and distributed by Aviso with support from CNES. The first author was granted a fellowship by the Spanish 'Ministerio de Ciencia e Innovación' during the development of her Ph.D. thesis. We would also like to thank David Sosa Trejo and Johan Sebastian Cortés Montenegro for their help, as well as all the scientific team and crew on board the BIO *Hespérides* for their hard work at sea during the ORCA cruise.

References

Alves, M., and A. Colin de Verdière (1999), Instability dynamics of a subtropical jet and applications to the Azores Front Current System: eddy-driven mean flow, *J. Phys. Oceanogr.*, *29*(5), 837–864.

Alves, M., F. Gaillard, M. Sparrow, M. Knoll, and S. Giraud (2002), Circulation patterns and transport of the Azores Front-Current system, *Deep Sea Res., Part II*, *49*(19), 3983–4002, doi:10.1016/S0967-0645(02)00138-8.

Arhan, M. (1990), The North Atlantic current and subarctic intermediate water, *J. Mar. Res.*, *48*(1), 109–144.

Arhan, M., A. De Verdière, and L. Mémery (1994), The eastern boundary of the Subtropical North Atlantic, *J. Phys. Oceanogr.*, *24*(6), 1295–1316.

Barbosa Aguiar, A., A. Peliz, A. Pires, and B. Le Cann (2011), Zonal structure of the mean flow and eddies in the Azores Current system, *J. Geophys. Res.*, *116*, C02012, doi:10.1029/2010JC006538.

Comas-Rodríguez, I., A. Hernández-Guerra, and E. McDonagh (2010), Referencing geostrophic velocities using ADCP data at 24.5°N (North Atlantic), *Sci. Mar.*, *74*(2), 331–338, doi:10.3989/scimar.2010.74n2331.

Cromwell, D., P. Challenor, A. New, and R. Pingree (1996), Persistent westward flow in the Azores Current as seen from altimetry and hydrography, *J. Geophys. Res.*, *101*(C5), 11,923–11,933.

Fiekas, V., J. Elken, T. Müller, A. Aitsam, and W. Zenk (1992), A view of the Canary Basin thermocline circulation in winter, *J. Geophys. Res.*, *97*(C8), 12,495–12,510, doi:10.1029/92JC01095.

Fischer, J., and M. Visbeck (1993), Deep velocity profiling with self-contained ADCPs, *J. Atmos. Oceanic Technol.*, *10*(5), 764–773.

Ganachaud, A. (2003), Large-scale mass transports, water mass formation, and diffusivities estimated from World Ocean Circulation Experiment (WOCE) hydrographic data, *J. Geophys. Res.*, *108*(C7), 3213, doi:10.1029/2002JC001565.

Gould, W. (1985), Physical oceanography of the Azores Front, *Prog. Oceanogr.*, *14*, 167–190, doi:10.1016/0079-6611(85)90010-2.

Hernández-Guerra, A., E. Fraile-Nuez, F. López-Laatzen, A. Martínez, G. Parrilla, and P. Vélez-Belchí (2005), Canary Current and North Equatorial Current from an inverse box model, *J. Geophys. Res.*, *110*, C12019, doi:10.1029/2005JC003032.

Jackett, D., and T. McDougall (1997), A neutral density variable for the world's oceans, *J. Phys. Oceanogr.*, *27*(2), 237–263.

Jia, Y. (2000), Formation of an Azores Current due to Mediterranean overflow in a modeling study of the North Atlantic, *J. Phys. Oceanogr.*, *30*, 2342–2358.

Käse, R., and W. Krauss (1996), The Gulf Stream, the North Atlantic Current, and the origin of the Azores current, in *The Warmwatersphere of the North Atlantic Ocean*, edited by W. Krauss et al., pp. 291–337, Borntraeger, Berlin.

Käse, R., and G. Siedler (1982), Meandering of the subtropical front southeast of the Azores, *Nature*, *300*, 245–246, doi:10.1038/300245a0.

Kida, S., J. Price, and J. Yang (2008), The upper-oceanic response to overflows: A mechanism for the Azores Current, *J. Phys. Oceanogr.*, *38*, 880–895.

Klein, B., and G. Siedler (1989), On the origin of the Azores Current, *J. Geophys. Res.*, *94*(C5), 6159–6168, doi:10.1029/JC094iC05p06159.

Lamas, L., Á. Peliz, I. Ambar, A. Barbosa Aguiar, N. Maximenko, and A. Teles-Machado (2010), Evidence of time-mean cyclonic cell southwest of Iberian Peninsula: The Mediterranean Outflow-driven β-plume?, *Geophys. Res. Lett.*, *37*, L12606, doi:10.1029/2010GL043339.

Machín, F., A. Hernández-Guerra, and J. Pelegrí (2006), Mass fluxes in the Canary Basin, *Prog. Oceanogr.*, *70*(2-4), 416–447, doi:10.1016/j.pocean.2006.03.019.

Martínez-Marrero, A., A. Rodríguez-Santana, A. Hernández-Guerra, E. Fraile-Nuez, F. López-Laatzen, P. Vélez-Belchí, and G. Parrilla (2008), Distribution of water masses and diapycnal mixing in the Cape

Verde Frontal Zone, *Geophys. Res. Lett.*, *35*, L07609, doi:10.1029/2008GL033229.

McDonagh, E., H. Bryden, B. King, and R. Sanders (2008), The circulation of the Indian Ocean at 32°S, *Prog. Oceanogr.*, *79*(1), 20–36, doi:10.1016/j.pocean.2008.07.001.

New, A., Y. Jia, M. Coulibaly, and J. Dengg (2001), On the role of the Azores Current in the ventilation of the North Atlantic Ocean, *Prog. Oceanogr.*, *48*(2-3), 163–194, doi:10.1016/S0079-6611(01)00004-0.

Onken, R. (1993), The Azores Countercurrent, *J. Phys. Oceanogr.*, *23*(8), 1638–1646.

Özgökmen, T., E. Chassignet, and C. Rooth (2001), On the connection between the Mediterranean outflow and the Azores Current, *J. Phys. Oceanogr.*, *31*(2), 461–480.

Paillet, J., and H. Mercier (1997), An inverse model of the eastern North Atlantic general circulation and thermocline ventilation, *Deep Sea Res., Part I*, *44*(8), 1293–1328, doi:10.1016/S0967-0637(97)00019-8.

Peliz, A., J. Dubert, P. Marchesiello, and A. Teles-Machado (2007), Surface circulation in the Gulf of Cadiz: Model and mean flow structure, *J. Geophys. Res.*, *112*, C11015, doi:10.1029/2007JC004159.

Pérez, F., M. Gilcoto, and A. Ríos (2003), Large and mesoscale variability of the water masses and the deep chlorophyll maximum in the Azores Front, *J. Geophys. Res.*, *108*(C7), 3215, doi:10.1029/2000JC000360.

Pingree, R., C. García-Soto, and B. Sinha (1999), Position and structure of the Subtropical/Azores Front region from combined Lagrangian and remote sensing (IR/altimeter/SeaWiFS) measurements, *J. Mar. Biol. Assoc. U.K.*, *79*(05), 769–792, doi:10.1017/S002531549900096X.

Smith, W., and D. Sandwell (1997), Global sea floor topography from satellite altimetry and ship depth soundings, *Science*, *277*(5334), 1956–1962, doi:10.1126/science.277.5334.1956.

Stramma, L. (1984), Geostrophic transport in the warm water sphere of the eastern subtropical North Atlantic, *J. Mar. Res.*, *42*(3), 537–558, doi:10.1357/002224084788506022.

Stramma, L., and T. Müller (1989), Some observations of the Azores Current and the North Equatorial Current, *J. Geophys. Res.*, *94*(C3), 3181–3186, doi:10.1029/JC094iC03p03181.

Stramma, L., and G. Siedler (1988), Seasonal changes in the North Atlantic subtropical gyre, *J. Geophys. Res.*, *93*(C7), 8111–8118, doi:10.1029/JC093iC07p08111.

Sy, A. (1988), Investigation of large-scale circulation patterns in the central North Atlantic: the North Atlantic Current, the Azores Current, and the Mediterranean Water plume in the area of the Mid-Atlantic Ridge, *Deep Sea Res.*, *35*(3), 383–413, doi:10.1016/0198-0149(88)90017-9.

Tychensky, A., P. Le Traon, F. Hernández, and D. Jourdan (1998), Large structures and temporal change in the Azores Front during the SEMAPHORE experiment, *J. Geophys. Res.*, *103*(C11), 25,009–25,027, doi:10.1029/98JC00782.

van Aken, H. (2000), The hydrography of the mid-latitude northeast Atlantic Ocean:: I: The deep water masses, *Deep Sea Res., Part I*, *47*(5), 757–788.

Volkov, D., and L. Fu (2010), On the reasons for the formation and variability of the Azores Current, *J. Phys. Oceanogr.*, *40*, 2197–2220, doi:10.1175/2010JPO4326.1.

V. M. Benítez-Barrios, E. Fraile-Nuez, and P. Vélez-Belchí, Instituto Español de Oceanografía, Centro Oceanográfico de Canarias, E-38001 Santa Cruz de Tenerife, Spain. (veronica.benitez@oceanografia.es; eugenio.fraile@oceanografia.es; pedro.velez@oceanografia.es)

I. Comas-Rodríguez, A. Hernández-Guerra, A. Martínez-Marrero, and M. D. Pérez-Hernández, Facultad de Ciencias de Mar, Universidad de Las Palmas de Gran Canaria, E-35017 Las Palmas, Spain. (isis.comas102@alu.ulpgc.es; ahernandez@dfis.ulpgc.es; amartinez@dfis.ulpgc.es; maria.perez263@alu.ulpgc.es)